The Effects of Narrowband Interference on OCDM

Muhammad Shahmeer Omar and Xiaoli Ma

School of Elec. and Computer Engr., Georgia Institute of Technology, Atlanta, GA 30332

Emails: {momar6, xiaoli}@gatech.edu

Abstract—Orthogonal chirp division multiplexing (OCDM) is a fairly new multi-carrier modulation scheme that has been proposed for optical fiber communications. It spreads data over an entire band using a set of linear chirps that are mutually orthogonal thus achieving the maximum spectral efficiency. This paper analyzes the performance of OCDM in wireless multi-path channels with narrow band interference (NBI) and in doing so shows that linear minimum mean squared error (MMSE) equalization exhibits an interesting signal-to-noise ratio (SNR) dependent degradation in error performance caused by interference amplification at high SNR. Furthermore, it employs a variant of the MMSE equalizer when the interference energy is known to prevent interference amplification and improve the error performance.

Index Terms—Orthogonal chirp division multiplexing, frequency domain equalization, narrowband interference.

I. Introduction

Orthogonal chirp division multiplexing (OCDM) is a relatively new multicarrier scheme that employs an orthogonal set of linear chirp signals as data carriers. As opposed to orthogonal frequency division multiplexing (OFDM), in which each symbol is transmitted using orthogonal subcarriers that partition the bandwidth, OCDM utilizes the entire signal bandwidth to transmit each symbol.

Currently, OFDM is the most widely used waveform as it enables low complexity equalization and is robust to multi-path fading. Moreover, OFDM and its multi-user variant orthogonal frequency division multiple access (OFDMA) enable high spectral efficiency by eliminating guard bands. However, OFDM has some well known problems, which include its inability to gather multi-path diversity and sensitivity to narrow band interference (NBI). In order to combat these problems, practical implementations, such as in long term evolution (LTE) networks [1] employ techniques that trade off spectral efficiency for performance gains. OCDM, being a spreading scheme promises to counter some of these problems.

OCDM was first proposed in [2] and it was shown that due to the relationship between the discrete Fresnel (DFnT) and discrete Fourier (DFT) transforms, it is possible to implement low complexity transceivers by leveraging the fast Fourier transform (FFT) algorithm. Moreover, the study proposed a low complexity frequency domain equalization (FDE) algorithm thus making the overall complexity of OCDM comparable to that of OFDM and single carrier with frequency domain

equalization (SC-FDE). Simulations showed that OCDM performs better than OFDM in multi-path channels with linear and decision feedback equalization but shows similar PAPR. Furthermore, OCDM was shown to be significantly more robust to interference caused by insufficient guard intervals than both OFDM and SC-FDE. However, this study did not characterize its performance in the presence of external interference.

The performance of OCDM in coherent optical fiber systems was investigated in [3] and a data rate of upto 112 Gbps was experimentally achieved using intensity modulation and direct detection. A continuous time analog of OCDM was proposed in [4] and it was shown that an arbitrary number of chirps from the chirp spread spectrum (CSS) can be multiplexed to maintain the orthogonality condition and asymptotically achieve the Nyquist rate. A pilot-based channel estimation scheme for coherent optical fiber OCDM was proposed in [5], in which an unmodulated Zadoff-Chu sequence was transmitted as a block pilot and was demodulated using an OCDM demodulator to directly compute the channel impulse response (CIR). Noise rejection windowing was subsequently used to improve the estimate quality. A combination of experiments and simulations were used to analyze the performance of OCDM in integrated fiber-wireless systems in the presence of narrow band interference (NBI) in [6] and OCDM was shown to perform better than OFDM when only a subset of chirps was used. However, this work does not specify the kind of channel and equalization used and does not consider channel coding.

In this paper, we study the impact of NBI on OCDM transmissions. Currently, the state-of-the art literature focuses on the performance of OCDM for optical fiber communications. Moreover, there is no work that analyzes the performance of OCDM in the presence NBI in multi-path channels with and without channel coding and with different linear equalizers. In doing so, we show that OCDM with linear minimum mean squared error (MMSE) equalization demonstrates performance degradation as the signal-to-noise ratio (SNR) increases in the presence of NBI. We use simulations and mathematical analysis, where possible, to describe the performance and use OFDM and SC-FDE as base-lines for comparison.

Common notations used in this paper include upper-case and lower-case bold letters such as $\mathbf{A}$ and $\mathbf{a}$ to denote matrices and vectors, respectively. The ith element of a vector $\mathbf{a}$ is denoted by $a(i)$ and the operators $(.)^{\mathcal{H}}$ and $(.)^T$ denote the hermitian and transpose, respectively. The DFT matrix is represented by $\mathbf{F}$ where $F(k,n) = \frac{1}{\sqrt{N}} e^{-j2\pi nk/N}$.

II. SYSTEM MODEL

Consider OCDM transmissions over multi-path channels in the presence of interference. At the transmitter, a parallel block of N symbols, taken from a complex modulation alphabet such as quadrature amplitude modulation (QAM) and given by $\mathbf{u}(i) = [u(iN), u(iN + 1), ..., u(iN + N - 1)]^T$, is modulated onto orthogonal chirps using the inverse discrete Fresnel transform (IDFnT). In block notation, this can be represented by $\mathbf{s} = \mathbf{\Phi}^{\mathcal{H}}\mathbf{u}$, where $\mathbf{\Phi}$ denotes an $N \times N$ DFnT matrix whose $(m, n)^{\text{th}}$ entry is given by [2]–[5]

$$\Phi(m, n) = \frac{1}{\sqrt{N}}e^{-j\frac{\pi}{4}} \times \begin{cases} e^{j\frac{\pi}{N}(m-n)^2} & N \equiv 0 \pmod 2 \\ e^{j\frac{\pi}{N}(m+\frac{1}{2}-n)^2} & N \equiv 1 \pmod 2. \end{cases} \tag{1}$$

A cyclic prefix (CP) of length N_{g} is appended to the resulting symbols before they are serialized, upconverted, amplified and transmitted. The transmitted block, of length $P = N + N_{\text{g}}$, is given by $\mathbf{x}(i) = \mathbf{T}_{\text{CP}}\mathbf{\Phi}^{\mathcal{H}}\mathbf{u}(i)$, where $\mathbf{T}_{\text{CP}} = [\mathbf{I}_{\text{CP}}^T \ \mathbf{I}_N^T]^T$ denotes the CP adding matrix and $\mathbf{I}_{\text{CP}}$ contains the last N_{g} rows of the identity matrix $\mathbf{I}_N$.

In this study, we consider a multi-path channel, whose impulse response is modeled by the vector $\mathbf{h} = [h(0), h(1), ..., h(L)]^T$, where the elements are zero-mean, independent complex normal random variables which is equivalent to a Rayleigh fading channel. Furthermore, we assume that the channel is quasi-static i.e., the CIR is constant for exactly one symbol duration. Therefore, the received OCDM signal, in the presence of interference is given by

$$\mathbf{y}(i) = \mathbf{H}_0\mathbf{x}(i) + \mathbf{H}_1\mathbf{x}(i - 1) + \tilde{\mathbf{v}}(i) + \tilde{\mathbf{w}}(i), \tag{2}$$

where $\tilde{\mathbf{w}}$ is an additive white Gaussian noise (AWGN) vector whose entries are i.i.d. complex normal random variables with a mean and variance of 0 and $\mathcal{N}_0$, respectively. The $P \times P$ matrices $\mathbf{H}_0$ and $\mathbf{H}_1$ are Toeplitz and are defined in [7] and $\tilde{\mathbf{v}}$ is a length-P column vector that denotes the interfering signal, which will be defined later. For the remainder of this study, we assume that $N_{\text{g}} \geq L$. Hence, there is no inter-block-interference (IBI) and the signal block, after downconversion, serial-to-parallel conversion and CP removal, is given by

$$\tilde{\mathbf{y}}(i) = \mathbf{R}_{\text{CP}}(\mathbf{H}_0\mathbf{T}_{\text{CP}}\mathbf{\Phi}^{\mathcal{H}}\mathbf{u}(i) + \mathbf{H}_1\mathbf{x}(i - 1) + \tilde{\mathbf{v}}(i) + \tilde{\mathbf{w}}(i)) \tag{3}$$

$$\stackrel{(a)}{=} \mathbf{H}\mathbf{\Phi}^{\mathcal{H}}\mathbf{u}(i) + \mathbf{v}(i) + \mathbf{w}(i), \tag{4}$$

where $\mathbf{R}_{\text{CP}} = [\mathbf{0}_{N \times N_g} \ \mathbf{I}_N]$ and (a) follows from the substitutions $\mathbf{H} = \mathbf{R}_{\text{CP}}\mathbf{H}_0\mathbf{T}_{\text{CP}}$, $\mathbf{R}_{\text{CP}}\mathbf{H}_1\mathbf{T}_{\text{CP}} = \mathbf{0}$, $\mathbf{v} = \mathbf{R}_{\text{CP}}\tilde{\mathbf{v}}$ and $\mathbf{w} = \mathbf{R}_{\text{CP}}\tilde{\mathbf{w}}$. Here, $\mathbf{H}$ is an $N \times N$ circulant matrix whose first column is given by $[\mathbf{h}^T \ \mathbf{0}_{N-L-1}^T]^T$.

To model the NBI, we adopt the definition from [8]. According to this, the nth sample of the tth interfering signal is given by

$$v_t(n) = \sqrt{\frac{E_I}{N}}e^{j(\frac{2\pi}{N}(m_t+\alpha)n+\theta_t)}, \quad 0 \leq n < N + N_g \tag{5}$$

where E_I is the energy of the interfering symbol, N is the total number of chirps available in the OCDM signal

or equivalently, the available subcarriers in OFDM, m_t is the frequency bin closest to the interfering signal, α is the position of the interference between frequency bins and θ_t is a uniform random variable such that $\theta_t \in [-\pi, \pi)$. For simplicity, we only consider the case when each interfering signal affects only one frequency bin, that is, $\alpha = 0$, noting that the impact on OCDM will not change when $\alpha \neq 0$. Assume there are $N_{\mathcal{A}}$ interfering signals, each occupying a different frequency bin and let $\mathcal{A} = \{t : m_t \in [0, N - 1]\}$ be the set of indices of active interferers. In this case, the interfering signal vector shown in Eq. (3) is given by $\tilde{\mathbf{v}} = [\sum_{t \in \mathcal{A}} v_t(0), \sum_{t \in \mathcal{A}} v_t(1), ..., \sum_{i \in \mathcal{A}} v_t(N + N_{\text{g}} - 1)]^T$.

It has been shown in [2] that OCDM allows for equalization in the frequency domain. Due to its lower complexity, we consider only linear frequency domain equalization (FDE) implemented through the zero-forcing (ZF) or MMSE criterion. Furthermore, we assume that the receiver has perfect knowledge of the CIR and the signal and noise variances. Letting $\mathbf{G}$ denote a general equalizer matrix, it follows that the recovered symbols are given by

$$\hat{\mathbf{u}} = \mathbf{F}^{\mathcal{H}}\mathbf{G}\mathbf{\Gamma}\mathbf{F}(\mathbf{H}\mathbf{\Phi}^{\mathcal{H}}\mathbf{u} + \mathbf{v} + \mathbf{w})$$
$$= \mathbf{F}^{\mathcal{H}}\mathbf{G}\mathbf{D}_h\mathbf{F}\mathbf{u} + \mathbf{F}^{\mathcal{H}}\mathbf{G}\mathbf{\Gamma}\mathbf{F}\mathbf{v} + \mathbf{F}^{\mathcal{H}}\mathbf{G}\mathbf{\Gamma}\mathbf{F}\mathbf{w}, \tag{6}$$

where $\mathbf{\Gamma} = \mathbf{F}\mathbf{\Phi}\mathbf{F}^{\mathcal{H}}$ is an $N \times N$ diagonal matrix with the nth entry on the main diagonal given by $e^{-j\pi n^2/N}$ when N is even and follows from the eigenvalue decomposition of the DFnT matrix. The $N \times N$ diagonal matrix $\mathbf{D}_h = \mathbf{F}\mathbf{H}\mathbf{F}^{\mathcal{H}}$ has the channel frequency response (CFR) on its main diagonal, given by $H(k) = \sum_n h(n)e^{-j2\pi kn/N}, \forall k \in [0, N - 1]$. Note that the received signal in Eq. (6) is independent of the block index i and thus the latter has been omitted.

III. PERFORMANCE DISCUSSION

In order to analyze the bit error rate (BER) behavior of OCDM, we resort to computing the mean squared error (MSE) of the symbol estimates, noting that when QPSK mapping is used, the BER in the lth subchannel is well approximated by [9]

$$\mathcal{P}_b(l) \approx Q\left(\sqrt{\frac{E_s}{\mathbb{E}\{|e(l)|^2\}}}\right), \tag{7}$$

where E_s is average symbol energy, $e(l)$ is the error on the lth subchannel and $\mathbb{E}\{|e(l)|^2\}$ is the MSE on the lth subchannel conditioned on the CIR. Considering the equalized symbols given by Eq. (6), it follows that the error is given by

$$\mathbf{e} = \hat{\mathbf{u}} - \mathbf{u}$$
$$= \mathbf{F}^{\mathcal{H}}(\mathbf{G}\mathbf{D}_h - \mathbf{I})\mathbf{F}\mathbf{u} + \mathbf{F}^{\mathcal{H}}\mathbf{G}\mathbf{\Gamma}\mathbf{F}\mathbf{v} + \mathbf{F}^{\mathcal{H}}\mathbf{G}\mathbf{\Gamma}\mathbf{F}\mathbf{w}, \tag{8}$$

where $\mathbf{G}$ is a diagonal matrix because the considered equalizer is a FDE. Hence, the error on the lth subchannel, given by the

l^{th} element of $\mathbf{e}$, can be expressed as

$$e(l) = e_1(l) + e_2(l) + e_3(l),$$

$$e_1(l) = \frac{1}{N} \sum_{k=0}^{N-1} (G(k)H(k) - 1)U(k)e^{j\frac{2\pi kl}{N}},$$

$$e_2(l) = \frac{1}{N} \sum_{k=0}^{N-1} G(k)\Gamma(k)V(k)e^{j\frac{2\pi kl}{N}},$$

$$e_3(l) = \frac{1}{N} \sum_{k=0}^{N-1} G(k)\Gamma(k)W(k)e^{j\frac{2\pi kl}{N}}, \qquad (9)$$

where $U(k)$, $V(k)$ and $W(k)$ are the kth element of the frequency response of $\mathbf{u}$, $\mathbf{v}$, and $\mathbf{w}$, respectively and are defined as $U(k) = \sum_n u(n)e^{-j2\pi nk/N}$. Here, we make a few observations about the expression in Eq. (9). First, the three error components are mutually independent as the transmitted and interfering signals and noise are independent. Second, we note that $\mathbb{E}\{V(k)V^\star(m)\} = 0$, $\mathbb{E}\{U(k)U^\star(m)\} = 0$ and $\mathbb{E}\{W(k)W^\star(m)\} = 0$ when $m \neq k$, which follows from the definition of the interfering signal in Eq. (5), and the fact that the noise samples and symbols are assumed to be independent. Incorporating these observations, the MSE on l^{th} subchannel, conditioned on the channel, is given by

$$\mathbb{E}\{|e(l)|^2\} = \mathbb{E}\{|e_1(l)|^2\} + \mathbb{E}\{|e_2(l)|^2\} + \mathbb{E}\{|e_3(l)|^2\}$$

$$= \frac{E_s}{N} \sum_{k=0}^{N-1} |G(k)H(k) - 1|^2 +$$

$$\left(\frac{N_{\mathcal{A}} E_I}{N^2} + \frac{\mathcal{N}_0}{N} \right) \sum_{k=0}^{N-1} |G(k)|^2. \qquad (10)$$

Eq. (10) gives us two insights into the behavior of OCDM: First, the MSE is independent of the subchannel index which means that all subchannels experience uniform degradation. Second, since the interferer exists only on a narrow band i.e., $N_{\mathcal{A}} < N$, the impact of the interference is mitigated as the demodulation process spreads the interference energy over the entire band.

When ZF equalization is used, the equalizer taps are given by $G(k) = 1/H(k)$ and the resulting MSE is given by

$$\mathbb{E}\{|e(l)|^2\} = \left(\frac{N_{\mathcal{A}} E_I}{N^2} + \frac{\mathcal{N}_0}{N} \right) \sum_{k=0}^{N-1} \frac{1}{|H(k)|^2}. \qquad (11)$$

It is easy to see that nulls on the spectral grid i.e., when $H(k) \approx 0$, will amplify both noise and interference. When MMSE equalization is used, the MSE is given by

$$\mathbb{E}\{|e(l)|^2\} = \frac{E_s}{N} \sum_{k=0}^{N-1} \left| \frac{|H(k)|^2}{|H(k)|^2 + 1/\rho} - 1 \right|^2 +$$

$$\left(\frac{N_{\mathcal{A}} E_I}{N^2} + \frac{E_s}{N\rho} \right) \sum_{k=0}^{N-1} \frac{|H(k)|^2}{(|H(k)|^2 + 1/\rho)^2}, \qquad (12)$$

where $\rho = E_s/\mathcal{N}_0$ denotes the input SNR Eq. (12) highlights the dependency of the MSE on the input SNR and shows

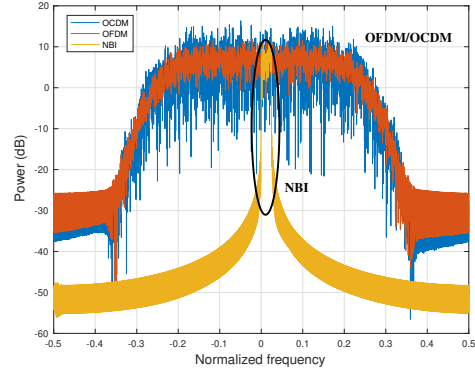Fig. 1. Power spectral densities of OFDM, OCDM and NBI signals when $N_{\mathcal{A}} = 100$ and all of the subchannels are being utilized.

TABLE I
EVA CHANNEL MODEL

Excess tap delay (ns)	0	30	150	310	370	710	1090	1730	2510
Relative power (dB)	0	-1.5	-1.4	-3.6	-0.6	-9.1	-7.0	-12.0	-16.9

that as ρ increases, the contribution of the noise and inter-symbol-interference (ISI) terms, indicated by the first and last sums, respectively, decreases but that of interference increases. Hence, as ρ increases, the interference becomes the dominant term and dictates the MSE and since it increases, so does the MSE, alluding to a deterioration in error performance as SNR increases beyond a certain threshold.

IV. NUMERICAL RESULTS

For all simulations, we consider both coded and uncoded transmissions with QPSK mapping, with $N = 2048$, in the presence of NBI. We assume a constraint length 7 and rate-1/3 convolutional code is used for the coded scenario and the coded bits are interleaved using a block interleaver. In the coded scenario, the transmission power is normalized by the code rate so that E_b/N_0 denotes the energy per data bit. All results are averaged over atleast 1000 channel realizations and the channel is assumed to have a power delay profile (PDP) given by the extended vehicular A (EVA) channel model. The relative path gains are given in Table. I. Fig. 1 shows the power spectral densities of the oversampled OCDM, OFDM and NBI signals when all of the subchannels are utilized for data. The oversampling factor was fixed at 2.

Fig. 2 compares the average BER of OCDM, OFDM and SC-FDE transmissions in the presence of NBI with different bandwidths and different equalization criterion. When ZF equalization is used, as shown in Fig. 2(a), OCDM and SC-FDE perform slightly worse than OFDM. e.g., at an SNR of 30 dB and when $N_{\mathcal{A}} = 50$, OFDM depicts a BER of 0.007 while SC-FDE and OCDM show a BER of 0.02. The performance of ZF equalization is limited by the noise and interference amplification in the presence of deep fades as shown in Eq. (11). In OFDM, this amplification only affects the subcarrier
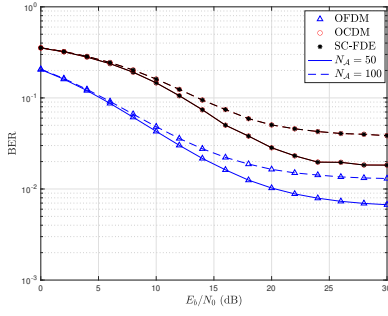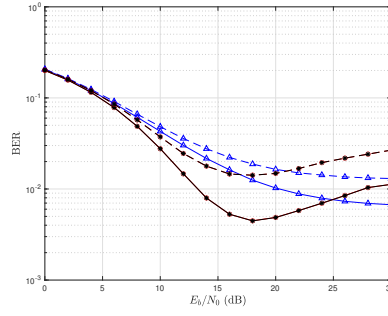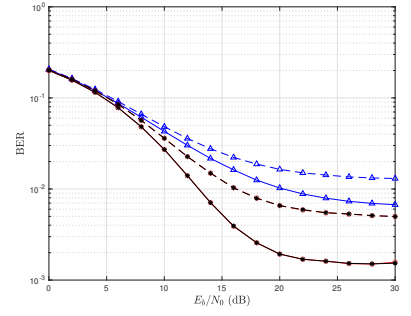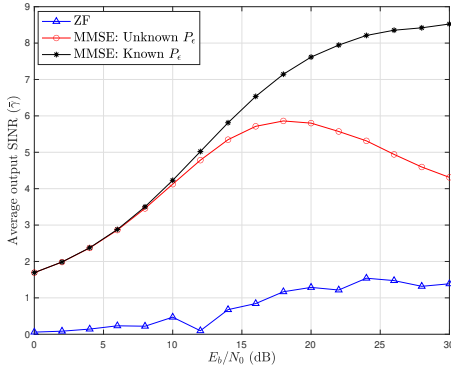
(a) ZF equalization   (b) MMSE equalization with unknown P_ϵ (c) MMSE equalization with known P_ϵ

Fig. 2. Average BER comparison of OFDM, OCDM and SC-FDE with different equalizers and when $N_\mathcal{A} = 50$ and $N_\mathcal{A} = 100$.

Fig. 3. Average SINR $\bar{\gamma}$ of the recovered OCDM symbols.

that experiences the deep fade. However, in OCDM, the resulting noise and interference amplification affects all the subchannels, leading to greater degradation than in OFDM.

Fig. 2(b) shows the BER of OCDM, SC-FDE and OFDM systems when MMSE equalization is used without knowledge of the interference power, denoted by P_ϵ. It can be seen that the BER initially decreases with increasing SNR and OCDM/SC-FDE outperforms OFDM. However, beyond a certain point the MMSE equalizer starts to amplify the interference and the BER starts to deteriorate. A similar trend was seen for SC-FDE systems in the presence of channel estimation errors in [9]. This does not occur for OFDM because unlike the other two schemes, each subcarrier in OFDM is independent and detection does not depend on the other subcarriers. This trend was predicted by Eq. (12) and can be explained by the fact that the standard MMSE equalizer does not minimize the MSE when interference is present. In order to remedy this, the knowledge of the interference energy must be incorporated and the kth tap of the resulting equalizer is given by

$$G(k) = \frac{H^\star(k)}{|H(k)|^2 + (P_\epsilon + \mathcal{N}_0)/E_s}. \tag{13}$$

The proof for this is fairly trivial and is thus omitted. Fig. 2(c) plots the BER of SC-FDE and OCDM systems with the modified MMSE equalizer and shows that there is no

longer any SNR dependent interference amplification. This is replaced by an error floor which is considerably lower than that of OFDM. For example, when $N_\mathcal{A} = 50$, OCDM/SC-FDE depicts a BER of approximately 10^{-3} and OFDM shows a BER of 0.007 at an SNR of 30 dB. However, increasing the interference bandwidth affects OCDM and SC-FDE more as it increases the MSE across all subchannels. However, in OFDM, the BER is simply limited by the number of subcarriers that experience interference or the ratio $N_\mathcal{A}/N$. Increasing the number of interferers does not significantly alter this ratio. Thus it has a relatively lower impact on OFDM.

Fig. 3 plots the argument to the function in Eq. (7), denoted as $\bar{\gamma}$, which can be defined as the average signal-to-noise-and-interference ratio (SINR) of the recovered symbols. It can be seen that the ZF equalizer shows the lowest output SINR due to noise and interference amplification. It also levels out earlier, which explains why OCDM and SC-FDE transmissions with ZF equalization encounter an error floor caused by the interference. However, when MMSE equalization is used, the output SINR increases with increasing input SNR initially but starts to decay as the SNR increases beyond a certain threshold. This mirrors the error profile shown in Fig. 2(b) and occurs because the MMSE equalizer starts to amplify interference when ρ is large. This problem can be circumvented by incorporating the knowledge of interference energy P_ϵ. Thus, the modified MMSE equalizer shows the highest output SINR, which begins to plateau at high SNR but does not show the same interference amplification as the MMSE equalizer which operates without knowledge of the interference energy. Consequently, the modified MMSE equalizer depicts an error floor, as shown in Fig. 2(c)

Fig. 4 plots the MSE for each subchannel in OFDM and OCDM transmissions with the modified MMSE equalizer. The first thing of note is that the MSE is constant across all subchannels in OCDM and eventually encounters a floor due to the interference. This is in stark contrast to the behavior of OFDM, where the subcarriers unaffected by the interference do not encounter this floor. However, the subcarriers that overlap with the NBI, as shown in Fig. 1, show very high MSE, thus rendering them un-decodeable. This greatly limits the average performance of OFDM.
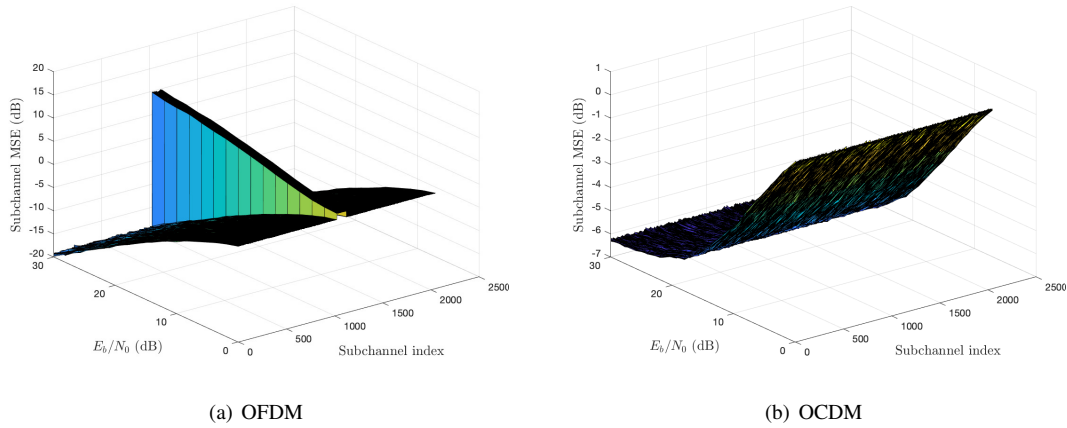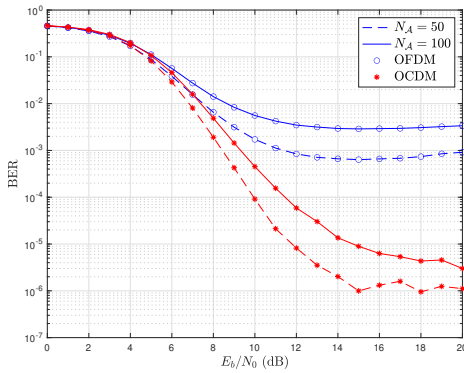
(a) OFDM

(b) OCDM

Fig. 4. MSE of OFDM and OCDM versus the SNR for all subchannels when $N_{\mathcal{A}} = 100$.

Fig. 5. Average BER of coded OFDM and OCDM.

Fig. 5 compares the performance of coded OCDM and OFDM. It is pertinent to note that since SC-FDE and OCDM have the same uncoded performance, it stands to reason that this will extend to the coded scenarios. Hence, we do not simulate coded SC-FDE. While offering gains in both schemes, the improvement afforded by channel coding to OCDM is considerably greater than to OFDM. For example, when E_b/N_0 is 20 dB and $N_{\mathcal{A}} = 50$, OFDM shows a BER of 10^{-3} and OCDM shows a BER of 10^{-6}. In OFDM, the data on the interfering subcarriers cannot be recovered and thus, there are too many errors for channel coding to effectively correct. This is not the case in OCDM as spreading evenly distributes errors and none of the subchannels are consistently un-decodeable. Hence, channel coding is more effective in OCDM in the presence of NBI.

V. CONCLUSIONS

In this paper, we analyzed the performance of OCDM in multi-path channels in the presence of NBI and compared it to the performances of OFDM and SC-FDE, two schemes which were chosen due to their technological relevance and similarities to OCDM, respectively. It was shown that OCDM

is more robust to NBI than OFDM, especially when knowledge of the interference energy is incorporated at the receiver. Moreover, it was shown that without this knowledge, MMSE equalizers amplified interference at high input SNRs leading to deterioration in reception quality. It was also shown that channel coding is not sufficient to correct for data lost on interfering subcarriers in OFDM. Thus, coded OCDM performed significantly better than its counterpart. However, SC-FDE and OCDM perform identically in the presence of NBI as they can both be considered spreading schemes, that is, each symbol in both schemes utilizes the entire bandwidth.

In the near future, we plan on extending this work to analyzing the performance of OCDM in fast and doubly selective fading channels and in the presence of CFO.

REFERENCES

[1] 3rd Generation Partnership Project (3GPP); Technical Specification Group Radio Access Network, "Evolved universal terrestrial radio access (E-UTRA) physical layer procedures (release 14)," *3GPP TS 36.212, V14.2.0.,* pp. 1–120, March 2017

[2] X. Ouyang and J. Zhao, "Orthogonal chirp division multiplexing," *IEEE Trans. Commun.*, vol. 64, no. 9, pp. 3946-3957, Sept. 2016.

[3] X. Ouyang and J. Zhao, "Orthogonal chirp division multiplexing for coherent optical fiber communications," *J. Lightw. Technol.*, vol. 34, no. 18, pp. 4376-4386, Sept.15, 2016.

[4] X. Ouyang, O. A. Dobre, Y. L. Guan, and J. Zhao, "Chirp spread spectrum toward the Nyquist signaling rate–orthogonality condition and applications," *IEEE Signal Process. Lett.,* vol. 24, no. 10, pp. 1488-1492, Oct. 2017.

[5] X. Ouyang, C. Antony, G. Talli and P. D. Townsend, "Robust channel estimation for coherent optical orthogonal chirp-division Multiplexing With pulse compression and noise rejection," *J. Lightw. Technol.,* vol. 36, no. 23, pp. 5600-5610, Dec.1, 2018.

[6] F. Lu, L. Cheng, M. Xu, J. Wang, S. Shen, and G. K. Chang, "Orthogonal chirp division multiplexing in millimeter-wave fiber-wireless integrated systems for enhanced mobile broadband and ultra-reliable communications," in *Proc. Optical Fiber Commun. Conf. (OFC)*, Los Angeles, CA, 2017, pp. 1-3.

[7] Z. Wang and G. B. Giannakis, "Wireless multicarrier communications," *IEEE Sig. Process. Mag.,* vol. 17, no. 3, pp. 29-48, May 2000.

[8] A. Batra and J. R. Zeidler, "Narrowband interference mitigation in OFDM systems," in *Proc. IEEE Military Commun. Conf.,* San Diego, CA, 2008, pp. 1-7.

[9] N. Souto, R. Dinis, and J. C. Silva, "Impact of channel estimation errors on SC-FDE systems," *IEEE Trans. Commun.*, vol. 62, no. 5, pp. 1530-1540, May 2014.